Journal of Sound and Vibration (2000) **233**(4), 573–585
doi:10.1006/jsvi.1999.2814, available online at http://www.idealibrary.com on IDEAL®

CALCULATION OF VIBRATORY POWER TRANSMISSION FOR USE IN ACTIVE VIBRATION CONTROL

C. Q. Howard, S. D. Snyder and C.H. Hansen

Department of Mechanical Engineering, The University of Adelaide, South Australia 5005, *Australia*

(*Received* 24 *March* 1998, *and in final form* 14 *September* 1999)

Typical active vibration isolation experiments use point measurements of acceleration or force at the junction between the vibratory source and the receiving structure. This does not necessarily lead to the minimization of the transmitted vibrational energy. A simple method is described to generate a signal which is proportional to the harmonic vibratory power transmission at the driving frequency, which is suitable for use as an error signal with an existing filtered-*x* feedforward active vibration controller.

1. INTRODUCTION

Vibratory power is a desirable cost function for active vibration control because it provides a true measure of the energy transmitted into a structure and thus its minimization will ensure a reduction in vibration levels throughout the structure. An attempt to reduce the transmitted power by only reducing the transmitted force or velocity amplitude, neglecting the relative phase angle, may not necessarily be successful in achieving global structural vibration reduction.

The method presented here was developed to enable the use of vibrational power transmission as a cost function with an existing digital active vibration controller. The controller used a feed-forward, filtered-*x*, least-mean-square (LMS), adaptive algorithm.

Vibratory power transmission can be measured by several methods. The two most common methods involve the use of an array of accelerometers mounted on the surface of the structure or a force–accelerometer pair. Both of these methods require some additional signal processing to combine the signals into a single meter.

The problem with using vibrational power transmission as a cost function with a typical LMS-type active vibrational controller is that the calculation of power results in a signal which is twice the frequency of the reference signal. Thus, the two signals are uncorrelated which means that the LMS algorithm will not perform the required cost function minimization.

Recent research [1] shows that point measurements of energy density, in the acoustic sense or structural intensity in the vibration sense, is a better measure of the global field, than point amplitude measurements of either squared acceleration (velocity) or force. The energy density in a structure is given by the difference of the power transmitted into the structure and the energy that is dissipated from the structure. The energy density in a structure is given by the summation of the potential energy and kinetic energy [2]. Hence reducing the power transmitted into a structure will reduce the potential and kinetic energy of a structure. In many cases, the purpose of vibration isolation is to reduce the noise radiated by the receiving structure [3, 4]. The energy in the receiving structure is available

0022-460X/00/240573 + 13 $35.00/0

to radiate noise [5] and hence reducing the energy in the receiving structure means that less energy is available to radiate noise. Pan *et al.* [6–8] applied this strategy to isolator systems and showed that it is possible to reduce the power transmission into a receiving structure. Many authors have also considered minimizing power transmission in one-dimensional [9–12] and two-dimensional structures [6, 13–21].

In a room, the total acoustic potential energy can be used as an active noise control cost function, and this is approximated as the sum of the squared pressures from suitably placed microphones [22]. Jenkins [23] used the analogy of the acoustic case to derive a cost function for the vibrational case; that is, the sum of the squared displacements of suitably placed accelerometers can be thought of as the vibrational potential energy. When Jenkins used an additional four accelerometers mounted on the plate to provide a better estimate of the vibrational potential energy, he found that the vibration attenuation improved by up to 10 dB. This suggests that he used an insufficient number of accelerometers to measure the global potential energy. This active vibration isolation experiment demonstrates that summation of squared acceleration at points on the structure can only approximate the global vibrational energy within a structure. An alternative method of measuring the global energy transmitted into a structure is to measure the vibrational energy which travels along the power transmission paths, which is called the structural intensity.

The literature shows that active control methods to minimize a global measure of vibrational energy will give superior results than minimization of point measurements of squared acceleration. However, it is difficult to practically measure the global vibrational energy in a structure. When a machine is vibrationally isolated from a receiving structure, the measurement of the power transmission at the interface of the vibrating source and the receiver is a practical method of measuring the global vibrational energy in the receiving structure.

It has been shown in the literature that in the calculation of vibrational power transmission (or structural intensity) at the intersection of an active isolator and support structure, the inclusion of power from rotational moments can act to cancel the contribution of power from translational forces [18, 24]. Power transmission from moments is converted into translational power transmission on reflection at the supports, and interacts with the translational power transmission resulting from translational forces. This can result in negative values of vibratory power transmission (that is, power reversal) along a translational axis [19, 20, 25].

Structural or acoustic intensity cost functions presented in the literature [10, 16, 26–31] attempt to minimize the signed value of structural intensity. All of these methods are based on a gradient descent algorithm to determine optimal filter coefficients which minimize the signed (not squared) value of the cost function. These algorithms are based on a cost function which consists of the total power transmission determined by measuring along a sufficient number of axes so that the cost function is positive definite. If negative values of measured power transmission are possible as a result of omitting the contribution of power transmission from motion around rotational axes or from phase errors in the measurements transducers, then the algorithms will converge to the negative value of translational power and could result in total power transmission (and thus overall structural vibration) levels which are greater than without control.

It follows that a better cost function to minimize is the absolute or squared value of power transmission rather than the signed value of power transmission. In the work described here, a method is presented which allows vibratory power or intensity to be used as a cost function which is positive definite, with a standard filtered-x LMS algorithm. This method is applied to the active isolation of vibrating rotating machinery from support structures. The primary source of vibratory power is always from the vibrating machine. The vibratory power is transmitted through an active vibration isolator which has a control actuator in parallel with a spring element. The support structure is assumed to have finite damping, which dissipates the vibratory power.

2. CALCULATION OF POWER

Consider a reference signal $x(t)$, a velocity signal $v(t)$ and a force signal $f(t)$ given by

$$x(t) = \mathrm{Re}(\hat{x}) = \mathrm{Re}(R\mathrm{e}^{\mathrm{j}\omega t}), \tag{1}$$

$$v(t) = \mathrm{Re}(\hat{v}) = \mathrm{Re}(V\mathrm{e}^{\mathrm{j}(\omega t+\theta)}), \tag{2}$$

$$f(t) = \mathrm{Re}(\hat{f}) = \mathrm{Re}(F\mathrm{e}^{\mathrm{j}(\omega t+\phi)}), \tag{3}$$

where $x(t)$ denotes a reference signal at a frequency ω, $f(t)$ the force, $v(t)$ the velocity. The quantities F and V are the real amplitudes of the force and velocity, respectively, and ϕ and θ are the phase angles of the force and velocity signals relative to the reference signal. Time-averaged vibratory power transmission P is given by the equation [32]

$$P = \langle fv \rangle_t = \tfrac{1}{2} FV \cos(\phi - \theta). \tag{4}$$

The transmission of vibratory power from a source structure into a receiving structure can be measured by mounting a force transducer at the connection point and an accelerometer next to the force transducer. The electrical signals from the transducers can be combined using an electronic (analog or digital) multiplier. The resulting signal will be proportional to the transmitted vibratory power.

3. MATHEMATICAL DERIVATION

First consider the product of a harmonic force signal $f(t)$ and a harmonic velocity signal $v(t)$. The result can be written as [33]

$$f(t)v(t) = \frac{FV}{2}[\cos(\theta - \phi) - \cos(2\omega t + \theta + \phi)]. \tag{5}$$

The terms in equation (5) consist of an oscillating component at twice the driving frequency and a constant term. The signal can be low-pass filtered to extract the constant term $(FV/2)\cos(\theta - \phi)$. This can be multiplied by the reference signal $x(t)$ to obtain a signal which is proportional to power transmission at the frequency of the reference signal:

$$P \propto \frac{RFV}{2}\cos(\theta - \phi)\sin(\omega t). \tag{6}$$

Equation (6) consists of an oscillating component at the driving frequency proportional to the transmitted vibratory power described in equation (4). This part of the signal may be used by the active vibration controller as the error signal. The error signal must be correlated with the reference signal as part of Wiener–Hopf conditions of the LMS algorithm (see reference [34] for a discussion on the LMS algorithm).

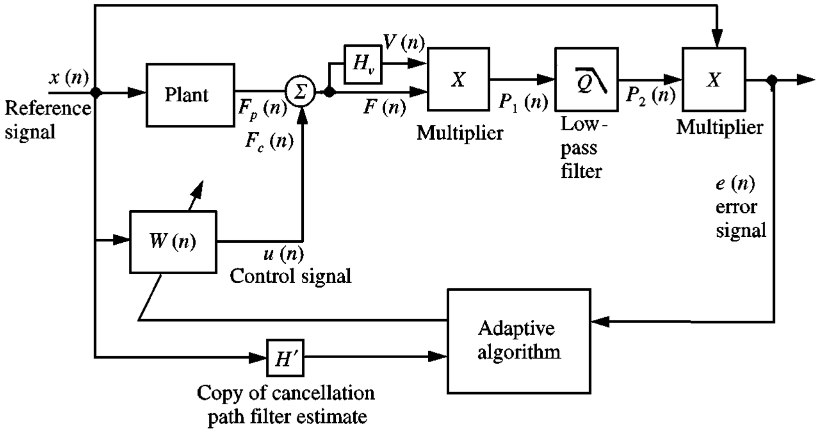

Figure 1. Control block diagram of a filtered-x LMS implementation using power transmission as an error signal.

The method described here is unsuitable for random signals as the filtering operation has a finite settling time before the correct constant signal proportional to power is obtained.

4. CONVERGENCE OF THE CONTROLLER

The multiplication and low-pass filtering method used to derive an error signal can be used in a conventional filtered-x LMS algorithm. A control block diagram for this case is shown in Figure 1.

A reference signal $x(n)$ is supplied to a plant which causes the structure to vibrate with a primary force response $\mathbf{F}_p(n)$ and a primary velocity response $\mathbf{V}_p(n) = \mathbf{H}_v * \mathbf{F}_p(n)$, where $*$ is the convolution operator. The reference signal is also provided to an adaptive controller $\mathbf{W}(n)$ which adapts slowly compared to the rate of change of the reference signal $x(n)$. The adaptive controller filters the reference signal to derive a control signal $u(n)$ given by

$$u(n) = \mathbf{W}(n) * \mathbf{X}(n), \tag{7}$$

where $\mathbf{W}(n)$ is a vector of the filter coefficients $w_i(n)$ and $\mathbf{X}(n)$ is a vector of past reference signal values $x(n)$. This control signal can be supplied to a control shaker which applies a counter-acting force to the structure. The control signal passes through the cancellation path which can be modelled by a transfer function $\mathbf{H}'$. The response of the control shaker power amplifiers, control shakers and error sensors (velocity and force) will be included in this cancellation path transfer function. The cancellation path filter can be determined while the controller is operating using another adaptive filter, or can be determined prior to implementing the controller. The velocity response is derived by multiplying the input force to the structure by a fixed transfer function $\mathbf{H}_v$ which is a function of the dynamics of the system. The error signal is derived from the product of the velocity response measurement and force response measurement as shown in Figure 1. The control signals and the primary signals will be additive such that the overall force response $\mathbf{F}(n)$ of the structure by the action of the primary and control sources is given by

$$\mathbf{F}(n) = \mathbf{F}_p(n) - \mathbf{W}(n) * \mathbf{X}(n). \tag{8}$$

The corresponding velocity response will be given by $\mathbf{V}(n) = \mathbf{H}_v * \mathbf{F}(n)$.

The force and velocity response of the structure are combined to obtain a measure of the power transmission. Following the procedure described in the previous section, the force and velocity signals are multiplied together such that

$$\mathbf{P}_1(n) = \mathbf{F}(n) * \mathbf{H}_v * \mathbf{F}(n). \tag{9}$$

The output from the first multiplier $\mathbf{P}_1(n)$ is then low-pass filtered to extract only the DC component of the signal. Practically, this is achieved by low-pass filtering with a cut off frequency around 10 Hz. A digital FIR filter (or IIR filter) is used which has filter weights given by the vector $\mathbf{Q}$ to yield

$$\mathbf{P}_2(n) = \mathbf{Q} * \mathbf{P}_1(n). \tag{10}$$

The low-pass filtered signal $\mathbf{P}_2(n)$ is then multiplied by the reference signal $\mathbf{X}(n)$ to obtain the error signal $e(n) = \mathbf{X}(n) * \mathbf{P}_2(n)$, the expected value of which is proportional to the power transmitted into the structure and at the reference signal frequency.

The error signal is the force and velocity signals which have been multiplied together and then low-pass filtered. The force signal $\mathbf{F}(n)$ is given by equation (8) and thus the product of the force and velocity is given by equation (9). When equation (8) is substituted into equation (9) and convolved with the low-pass filter $\mathbf{Q}$ we obtain the following:

$$e(n) = \mathbf{X} * \mathbf{Q} * \mathbf{H}_v * (\mathbf{F}_p(n) - \mathbf{W} * \mathbf{X}) * (\mathbf{F}_p(n) - \mathbf{W} * \mathbf{X})^{\mathrm{T}} \tag{11}$$

$$= \mathbf{X} * \mathbf{Q} * \mathbf{H}_v * \mathbf{F}(n) * [\mathbf{F}(n)]^{\mathrm{T}}. \tag{12}$$

The cost function used by the conventional filtered-x LMS algorithm is given by $J = E[e(n)^2]$, where E is the statistical expectation operator. Substitution of equation (12) into the cost function gives

$$J = E[(\mathbf{X} * \mathbf{Q} * \mathbf{H}_v * \mathbf{F}(n) * [\mathbf{F}(n)]^{\mathrm{T}})(\mathbf{X} * \mathbf{Q} * \mathbf{H}_v * \mathbf{F}(n) * [\mathbf{F}(n)]^{\mathrm{T}})^{\mathrm{T}}]. \tag{13}$$

Equation (13) is a quartic function of the filter weights. The error surface is bowl shaped and always positive. Hence, conventional gradient descent algorithms such as the filtered-x LMS algorithm will converge to the global minimum.

5. EXPERIMENTAL INVESTIGATION

The method of generating an electrical signal proportional to the vibratory power was experimentally investigated by measuring the power transmission into a simply supported beam.

The multiplication and low-pass filtering of the signals may be achieved by using either analog or digital circuitry. The first attempt at implementing the method used an analog circuit. Two integrated circuits were used (EXAR XR2208), a Rockland filter and a voltage amplifier. Each integrated circuit multiplied two input signals and attenuated the resulting signal by 20 dB. The input signals to one of the multiplier circuits were the velocity and force signals. The output from the multiplier was low-pass filtered below 30 Hz to obtain the DC component of the electrical signal. When the signal level was low, a voltage amplifier capable of amplification of DC signals was used to increase the signal level by 20 dB. This was important as the DC component of the first stage multiplication process is used in the second stage. The output from the first stage was fed into the second multiplier with the reference signal. This resulted in a signal which was proportional to the expected

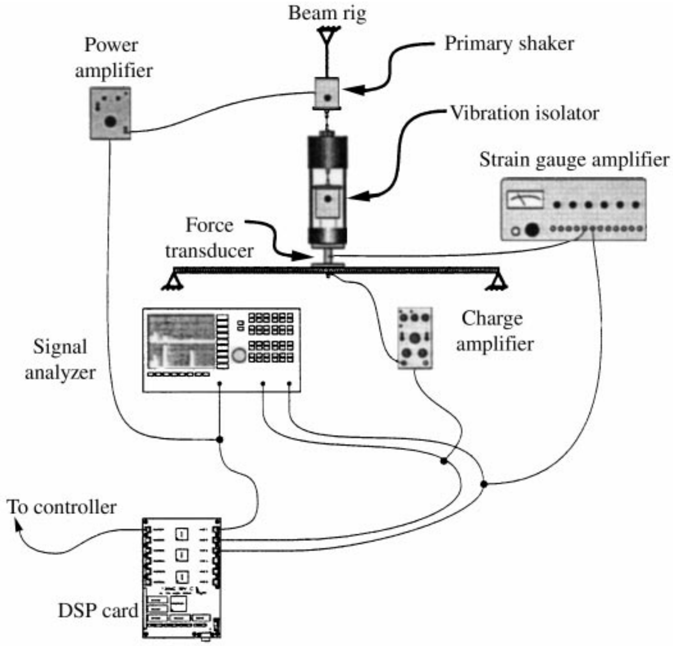

Figure 2. Equipment set-up.

value of vibrational power at the frequency of the reference signal. However, the analog circuit had a poor signal-to-noise ratio. When the signal levels were low, the circuit behaved non-linearly and the resulting signal was not proportional to the vibratory power. For lightly damped structures, the force and velocity signals are close to 90° apart in phase, which means that the cosine of the phase difference is close to zero. This results in low signal amplitudes and hence difficulties with the linearity of the circuitry.

The multiplication and low-pass filtering was also implemented using a digital signal processing (DSP) board made by Causal Systems. The inputs to the DSP board were the reference, velocity and force signals. The algorithm implemented on the DSP board multiplied the force and velocity signals and performed a digital low-pass filtering operation using a 4-tap IIR filter with the 3 dB point at 20 Hz. The output of the filter was digitally amplified by digital bit shifting. The resulting signal was constant and this was multiplied by the reference signal. The result was written to the output channel of the DSP board. This signal was proportional to the vibratory power transmission at the frequency of the reference signal. The signal-to-noise ratio of this system was significantly better than the analog circuit and thus this system was used to obtain the experimental results.

Figure 2 illustrates the equipment used to verify the heterodyning technique described above. The figure shows a primary shaker connected to a large mass which is connected to a vibration isolator. The vibration isolator is attached to the beam with a force transducer between the isolator and the beam. The simply supported beam had dimensions of 25 mm square and 1500 mm length between the supports. An accelerometer at the base of the isolator was used to measure the velocity of the beam at the junction. The vibration isolator was located at the center of the beam.

The power transmitted into the beam was measured by using a strain gauge force transducer and a Bruel and Kjær-type 4393 accelerometer. A Bruel and Kjær-type 2635 charge amplifier was used to condition the acceleration signal and a strain gauge amplifier

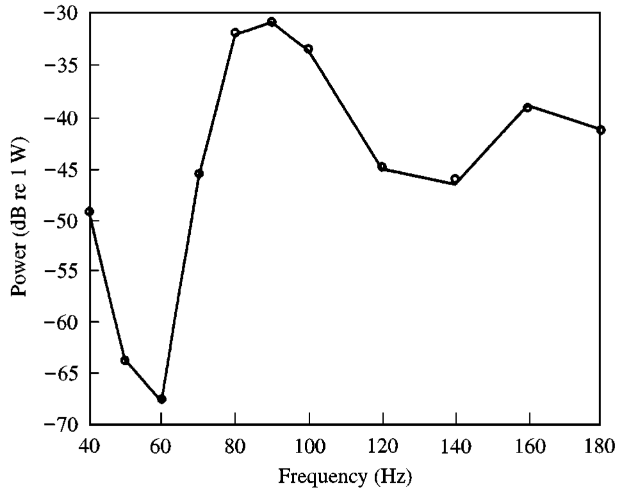

Figure 3. Comparison of measured vibratory power and heterodyned signals. ——, HP analyzer; ○, digital multiplier & low pass filter.

was used to condition the signal from the force transducer. The acceleration signal was integrated using the charge amplifier to obtain a velocity signal. The force, velocity and reference signals were supplied to the DSP board. The vibratory power was also calculated using equation (4) implemented on a Hewlett-Packard 35665A signal analyzer.

The signal analyzer provided a sinusoidal signal for the power amplifier to drive the shaker and a reference signal for the DSP board.

The test involved comparing the calculated power transmission with the output of the DSP board over a frequency range of 140 Hz.

Figure 3 shows the comparison of the peak voltages at the driving frequency from the DSP board with the calculated vibratory power transmission using equation (4). Measurements were taken over a frequency range from 40 to 180 Hz. The voltage values from the DSP board were shifted by 22 dB so that the points would lie on top of the calculated vibratory power transmission. This scaling operation does not affect the operation of the active vibration controller as all that is required is a signal which is proportional to vibratory power transmission.

Figure 3 thus shows that the heterodyned signal is proportional to the measured power transmission and is a suitable error signal for a filtered-x LMS adaptive controller.

5.1. ACTIVE CONTROL EXPERIMENT

The purpose of this experiment was to confirm that the heterodyning technique described above could be used in conjunction with a filtered-x LMS adaptive controller to minimize the squared power transmission P_z^2 along the vertical axis.

The instrumentation that was used in the experiment is shown in Figure 4. Velocity signals were obtained by integrating the acceleration signals from the accelerometers attached to the force transducer, using the analog integrator on the B&K 2635 charge amplifiers. The heterodyning technique was programmed in assembly language to run on a DSP board. The force, velocity and reference signals were supplied to the input channels of the DSP board, which multiplied the force and velocity signals together, performed

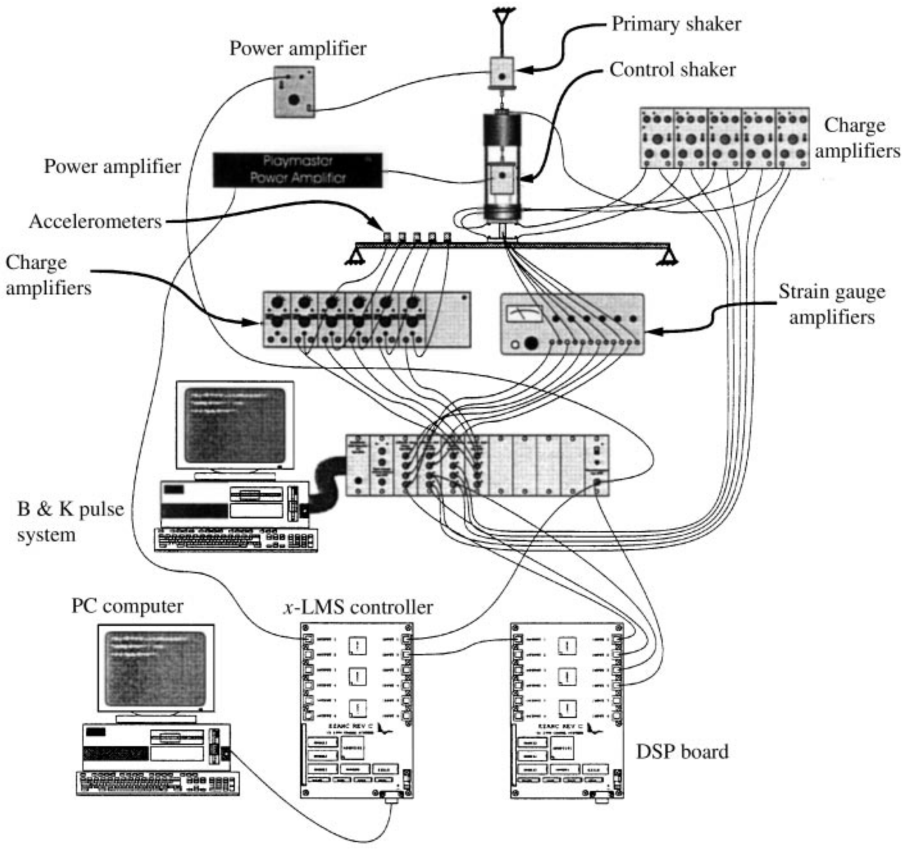

Figure 4. Instrumentation used in the adaptive control experiment which uses the heterodyning technique.

a low-pass filter on the resulting signal using a 4-tap IIR filter with the 3 dB point at 20 Hz, then multiplied the low-pass filtered signal by the reference signal and output the resulting signal. The output signal from the DSP board was connected to a conventional filtered-x LMS controller, which in this case was an EZ-ANC active noise controller produced by Causal Systems.

The vibration isolation performance was determined by the change in approximate kinetic energy (KE) of the beam measured by summing the squared accelerations of five accelerometers mounted at 0·30, 0·35, 0·45 and 0·50 m from the end of the beam. This measurement is not affected by phase errors and provides a reasonable approximation of the global KE of the beam. It also provides an independent measure of the isolation performance. Comparisons of the isolation performance using a single sensor, for example the acceleration at the base of the isolator, does not provide a good measure because it is possible to minimize the vibration at the sensor and increase the vibration elsewhere on the supporting structure. The true value of the KE requires the summation of an infinite number of acceleration measurements over the length of the beam to measure the translational and rotational accelerations.

The experimental measurements of the vibration isolation performance are derived using two methods. The first method uses measured transfer function data to calculate the appropriate control force to minimize the chosen cost function. This method assumes that a perfect active vibration controller is available. The second method uses a commercially available filtered-x LMS adaptive controller and a second DSP board to implement the heterodyning technique described above.

5.2. TRANSFER FUNCTION METHOD TO PREDICT THE VIBRATION ISOLATION USING ACTIVE CONTROL

The method of using measured transfer function data to predict the active control performance has been considered previously for acoustic systems [35, 36] where measured acoustic transfer function data were used to predict the sound pressure levels inside an aircraft cabin for active noise control.

Transfer functions are measured between the driving force on the structure and the response at the error sensors. The driving force is measured by placing a force transducer between a shaker and the structure. Response measurements are made at the force transducer between the isolator and the beam, and the accelerometers which measure the acceleration of the structure. Transfer functions are measured between the primary shaker and the error sensors and between the control shakers and the error sensors.

The error signals from the error sensors can be written in matrix form as [37, Appendix A.5]

$$\mathbf{e} = \mathbf{d} + \mathbf{C}\mathbf{x}, \tag{14}$$

where $\mathbf{e}$ is an $(n_e \times 1)$ vector of n_e error signals, $\mathbf{x}$ is an $(n_c \times 1)$ vector of control signals, $\mathbf{d}$ is an $(n_e \times 1)$ vector of the error signals resulting from passive control and $\mathbf{C}$ is an $(n_e \times n_c)$ matrix of the transfer functions between the control signals and the error signals when the primary disturbance is turned off. The usual goal of active control systems is to determine the amplitude and phase of the control signals which will cancel the primary disturbance, and is given by the re-arrangement of equation (14) as

$$\mathbf{x}_0 = -(\mathbf{C})^{-1}\mathbf{d}. \tag{15}$$

Equation (15) can be solved when there are an equal number of control signals and error signals ($n_c = n_e$). When there are an unequal number of control signals and error signals a least-mean-square approach can be used [37].

Consider the system shown in Figure 4 where the velocity along the vertical axis at the base of the isolator is to be minimized when the top rigid body is subjected to a harmonic vertical primary force. There is one error sensor and one control force ($n_e = n_c = 1$), and hence equation (15) can be used to determine the optimal control force. A transfer function measurement is taken over the frequency range of interest, between the primary driving force and the velocity along the vertical axis at the base of the isolator and this transfer function is called $\mathbf{Z}_{vp}$. The primary driving force is then turned off and a transfer function measurement is taken between the force exerted by the control shaker and the velocity along the vertical axis at the base of the isolator, and this transfer function is called $\mathbf{Z}_{vc}$. The terms $\mathbf{d}$ and $\mathbf{C}$ become

$$\mathbf{d} = \mathbf{Z}_{vp}\mathbf{f}_p, \qquad \mathbf{C} = \mathbf{Z}_{vc}, \tag{16, 17}$$

where $\mathbf{f}_p$ is the $(n_p \times 1)$ column vector of primary forces, which for this example is $\mathbf{f}_p = 1$.

In the experiments where squared power transmission is minimized, the error surface of filter weight values versus mean-square error does not exhibit the typical paraboloid shape.

The presence of small moments at the intersection of the isolator and beam generates negative values of power transmission along the vertical axis. Hence, the error surface resembles a paraboloid with an inverted bowl at the center of the paraboloid, where the signed value of power transmission along the vertical axis is negative [25, 38]. To minimize the squared value of power transmission, a different method of adaptation is required to guide the search process towards the minimum value of the cost function. The strategy involves starting the adaptation process from the minimization of the squared acceleration along the vertical axis [39].

5.3. RESULTS

Figure 5 shows the approximate KE of the beam for the minimization of squared acceleration along the vertical Z-axis and the minimization of squared power transmission along the vertical Z-axis, when using the transfer function method and an adaptive controller. The frequency range of interest is between 0 and 200 Hz which corresponds to the first three vibration modes of the beam. Figure 5 shows that minimizing squared power transmission along the vertical Z-axis performs as well as minimizing squared acceleration along the vertical Z-axis in terms of controlling the power transmission through the isolator into the beam. This demonstrates that the heterodyning technique can be used to generate an error signal proportional to the mean power transmission thus allowing real-time minimization of the power transmission into the beam.

The filtered-x LMS controller converged extremely slowly and was unstable when minimizing the squared power transmission along the vertical axis. The filtered-x LMS algorithm uses an adaptive filter to model the transfer function between a signal that is injected at the control shaker and the resulting error signal. This model is called the

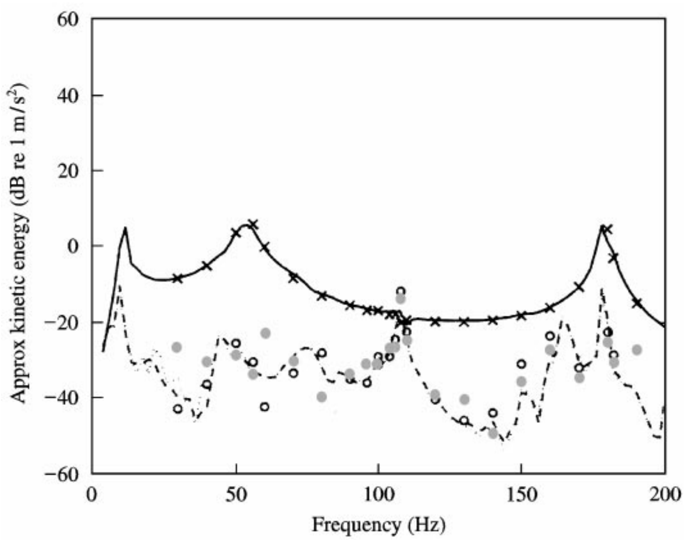

Figure 5. Experimental results of the KE of the beam for passive isolation, minimization of squared acceleration A_z^2 along the vertical axis, minimization of squared power transmission P_z^2 along the vertical axis using the transfer function method and the adaptive controller. —— Passive: xfer method; × × Passive: measured; – – – Active: Min Az^2 xfer method; ··· Active: Min Pz^2 xfer method; ○ Active: Min Az^2 controller; ● Active: Min Az^2 controller.

cancellation path transfer function model. In this case, the error signal was the squared power transmission which was derived using the heterodyning technique and it was not possible to obtain a good model in this experiment, which is the cause of the poor convergence and instability of the controller. It can be seen from equation (12), that the error signal $e(n)$ is a cubic function of the reference signal $x(n)$, which means that the formula for the error signal is a non-linear function. The cancellation path transfer function is assumed to be a linear transfer function and the controller is therefore not able to model the non-linear transfer function accurately. Attempts were made to improve the cancellation path transfer function model by using a long filter length (100 taps), but this did not improve the stability of the system. Another attempt was made to improve the stability by replacing the filtered-x LMS controller with an LMS controller which was programmed on the DSP board. The LMS algorithm is almost the same as the filtered-x LMS algorithm except that the cancellation path transfer function is not used. The use of the LMS controller did not improve the stability of the system.

Further research would be required to improve the stability of the controller when using the heterodyning technique and this is beyond the intended scope of this paper.

6. CONCLUSIONS

A method of combining velocity and force signals has been described which provides a signal proportional to mean vibrational power transmission at the driving frequency. This signal is suitable for use as a cost function in a feedforward active vibration controller. An experiment was performed to verify that the method provides a signal proportional to power for various power levels and for various frequencies. The results showed that the method was accurate in all cases.

An experiment was conducted to demonstrate that an adaptive controller, which uses a filtered-x LMS algorithm, could be used to minimize the squared power transmission into the beam along the vertical axis. The heterodyning technique, which was described here, was used to generate an error signal that was proportional to squared power transmission. The isolation performance when the squared power transmission was minimized was about the same as when the squared acceleration or squared velocity was minimized. However, the adaptive controller was unstable when using the error signal generated by the heterodyning technique, caused by the inability of the cancellation path transfer function filter to model the non-linear error signal. The experiment also verified that the same results could be obtained by using the transfer function method or by using an adaptive controller.

This work has demonstrated a method to calculate an error signal that is proportional to the mean vibratory power transmission at the same frequency as the driving frequency.

REFERENCES

1. Y. C. Park and S. D. Sommerfeldt 1997 *Journal of the Acoustical Society of America* **101**, 350–359. Global attenuation of broadband noise fields using energy density control.
2. O. Bouthier, R. Bernhard and C. Wohlever 1990 *Proceedings of the 3rd International Congress on Intensity Techniques, Senlis, France*, 37–43. Energy and structural intensity formulations of beam and plate vibrations.
3. A. T. Moorhouse and B. M. Gibbs 1993 *Journal of Sound and Vibration* **167**, 223–237. Prediction of the structure borne noise emission of machines: development of a methodology.
4. C. R. Fuller and E. Toffin 1994 *Proceedings of the 127th Meeting of the Acoustical Society of America, Massachusetts Institute of Technology, Cambridge, MA*, Vol. 5aNS1, 2987–2988. *Session 5aNS: Noise and Structural Acoustics and Vibration: Active Noise and Vibration Control.* Passive–active isolator control of sound radiation from a raft–cylinder system.

5. A. T. MOORHOUSE and B. M. GIBBS 1995 *Acoustic Bulletin* 21–26. Structure borne sound—the unheard acoustic.
6. J. Q. PAN and C. H. HANSEN 1993 *Journal of the Acoustical Society of America* **93**, 1947–1953. Active control of vibratory power flow from a vibrating rigid body to a flexible panel through two active isolators.
7. J. Q. PAN, C. H. HANSEN and J. PAN 1991 *Proceedings of InterNoise* '91, 683–686. Sydney, Australia: Australian Acoustical Society. Active isolation of a vibration source from a thin beam using a single active mount.
8. J. Q. PAN, C. H. HANSEN and J. PAN 1993 *Journal of the Acoustical Society of America* **94**, 1425–1434. Active isolation of a vibration source from a thin beam using a single active mount.
9. D. W. MILLER, S. R. HALL and A. VON FLOTOW 1990 *Journal of Sound and Vibration* **140**, 475–497. Optimal control of power flow at structural junctions.
10. A. E. SCHWENK, S. D. SOMMERFELDT and S. I. HAYEK 1994 *Journal of the Acoustical Society of America* **96**, 2826–2835. Adaptive control of structural intensity associated with bending waves in a beam.
11. W. REDMAN-WHITE, P. A. NELSON and A. R. D. CURTIS 1987 *Journal of Sound and Vibration* **112**, 187–191. (Letters to the Editor). Experiments on the active control of flexural wave power flow.
12. G. P. GIBBS and C. R. FULLER 1990 *AIAM SDM Conference*, *Long Beach*, *California*, *U.S.A*. Experiments on active control of vibrational power flow using piezoceramic actuators and sensors.
13. Y. K. KOH and R. G. WHITE 1997 *Journal of Sound and Vibration* **196**, 469–493. Analysis and control of vibrational power transmission to machinery supporting structures subjected to a multi-excitation system, Part I: driving point mobility matrix of beams and rectangular plates.
14. Y. K. KOH and R. G. WHITE 1997 *Journal of Sound and Vibration* **196**, 495–508. Analysis and control of vibrational power transmission to machinery supporting structures subjected to a multi-excitation system, Part II: vibrational power analysis and control schemes.
15. Y. K. KOH and R. G. WHITE 1997 *Journal of Sound and Vibration* **196**, 509–522. Analysis and control of vibrational power transmission to machinery supporting structures subjected to a multi-excitation system, Part III: vibrational power cancellation and control experiments.
16. M. NAM, S. I. HAYEK and S. D. SOMMERFELDT 1995 *Proceedings of the Active* '95, 209–220. *Newport Beach*, *CA*, *U.S.A*., *July*. *Institute of Noise Control Engineering*. New York, U.S.A.: Noise Control Foundation. Active control of structural intensity in connected structures.
17. J. PAN, J. Q. PAN and C. H. HANSEN 1992 *Journal of the Acoustical Society of America* **92**, 895–907. Total power flow from a vibrating rigid body to a thin panel through multiple elastic mounts.
18. P. GARDONIO, S. J. ELLIOT and R. J. PINNINGTON 1995 *ISVR Technical Memorandum* 765, *Institute of Sound and Vibration*. Active isolation of multiple-degree of freedom vibrations transmission between a source and a receiver.
19. P. GARDONIO, S. J. ELLIOT and R. J. PINNINGTON 1997 *Journal of Sound and Vibration* **207**, 61–93. Active isolation of structural vibration on a multiple degree of freedom system, Part I: the dynamics of the system.
20. P. GARDONIO, S. J. ELLIOT and R. J. PINNINGTON 1997 *Journal of Sound and Vibration* **207**, 95–121. Active isolation of structural vibration on a multiple degree of freedom system, Part II: effectiveness of active control strategies.
21. O. BARDOI, P. GARDONIO, S. J. ELLIOT and R. J. PINNINGTON 1997 *Journal of Sound and Vibration* **208**, 111–151. Active power minimization and power absorption in a plate with force and moment excitation.
22. P. A. NELSON, A. R. D. CURTIS, S. J. ELLIOTT and A. J. BULLMORE 1987 *Journal of Sound and Vibration* **117**, 1–13. The active minimization of harmonic enclosed sound fields. Part I: theory.
23. M. D. JENKINS 1989 *Ph.D. Thesis*, *University of Southhampton*. Active control of periodic machinery vibrations.
24. Y. K. KOH and R. G. WHITE 1996 *Journal of Sound and Vibration* **196**, 495–508. Analysis and control of vibrational power transmission to machinery supporting structures subjected to a multi-excitation system, Part II: vibrational power analysis and control schemes.
25. C. Q. HOWARD and C. H. HANSEN 1999 *International Journal of Acoustics and Vibration* **4**, 23–36. Finite element analysis of active vibration isolation using vibrational power as a cost function.

26. J. HALD 1991 *International Symposium on Active Control of Sound and Vibration, Tokyo, Japan, April*, 285–290. *Acoustical Society of Japan.* Tokyo, Japan: Acoustical Society of Japan. A power controlled active noise cancellation technique.
27. K. M. REICHARD, D. C. SWANSON and S. M. HIRSCH 1995 *Proceedings of the Active* 95, *Newport Beach, CA, U.S.A., July*, 395–406. *Institute of Noise Control Engineering*. New York, U.S.A.: Noise Control Foundtion. Control of acoustic intensity using the frequency domain filtered-x algorithm.
28. S. D. SOMMERFELDT and P. J. NASHIF 1994 *Journal of the Acoustical Society of America* **96**, 300–306. An adaptive filtered-x algorithm for energy based active control.
29. E. HENRIKSEN 1996 *Proceedings of the Inter-Noise* 96, *Liverpool, England*, 1615–1618. International Congress on Noise Control Engineering. St Albàns, U.K.: Institute of Acoustics. Adaptive active control of structural vibration by minimisation of total supplied power.
30. S.-W. KANG and Y.-H. KIM 1997 *Journal of Sound and Vibration* **201**, 595–611. Active intensity control for the reduction of radiated duct noise.
31. D. C. SWANSON, C. A. GENTRY, S. I. HAYEK and S. D. SOMMERFELDT 1997 *The Journal of the Acoustical Society of America* **101**, 623–625. An error intensity spectral filtering method for active control of broadband structural intensity.
32. E. SKUDRZYK 1968 *Simple and Complex Vibratory Systems*. U.S.A., The Pennsylvania State University Press.
33. F. J. FAHY 1995 *Sound Intensity*. London: E & F Spon, second edition.
34. B. WIDROW and S. D. STEARNS 1985 *Adaptive Signal Processing*. Englewood Cliffs, NJ: Prentice-Hall.
35. C. M. DORLING, G. P. EATWELL, S. M. HUTCHINS, C. F. ROSS and S. G. C. SUTCLIFFE 1987 *Journal of Sound and Vibration* **112**, 389–395. A demonstration of active noise reduction in an aircraft.
36. C. M. DORLING, B. P. EATWELL, S. M. HUTCHINS, C. F. ROSS and S. G. C. SUTCLIFFE 1989 *Journal of Sound and Vibration* **128**, 358–360. A demonstration of active noise reduction in an aircraft cabin.
37. P. A. NELSON and S. J. ELLIOTT 1992 *Active Control of Sound*. San Diego: Academic Press.
38. C. Q. HOWARD and C. H. HANSEN 1997 *Proceedings of Fifth International Congress on Sound and Vibration, Adelaide, South Australia, Australia, December*, 421–427. Finite element analysis of active vibration isolation.
39. C. Q. HOWARD (1999) *Ph.D. Thesis, University of Adelaide, Australia.* Active isolation of machinery vibration from flexible structures.